Cell

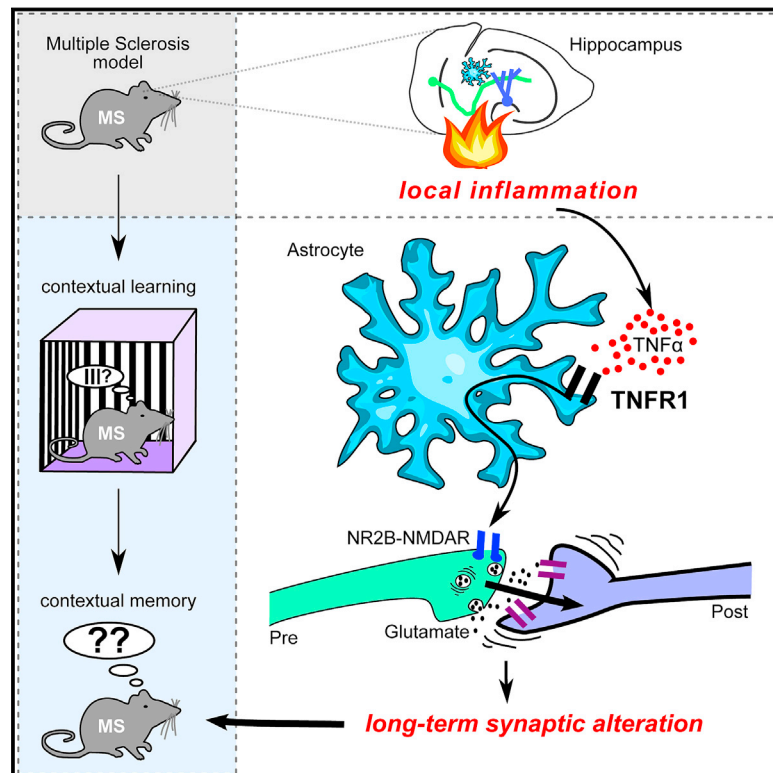# Neuroinflammatory TNFα Impairs Memory via Astrocyte Signaling

Graphical Abstract

Authors

Samia Habbas, Mirko Santello, Denise Becker, ..., Christopher R. Pryce, Tobias Suter, Andrea Volterra

Correspondence

andrea.volterra@unil.ch

In Brief

Pathological levels of TNFα trigger signaling in astrocytes, leading to synaptic alterations and memory deficits in a mouse model of multiple sclerosis.

Highlights

- Pathological levels of TNFα cause persistent synaptic alteration in the hippocampus

- Astrocyte TNFR1 mediates the synaptic effect of TNFα

- Hippocampal inflammation and synaptic alteration occur in a multiple sclerosis model

- Astrocyte TNFR1 is necessary for synaptic alterations and ensuing cognitive pathology

CellPress

Article

Cell

Neuroinflammatory TNFα Impairs Memory via Astrocyte Signaling

Samia Habbas,[1,6] Mirko Santello,[1,6,7] Denise Becker,[1] Hiltrud Stubbe,[1] Giovanna Zappia,[1] Nicolas Liaudet,[1] Federica R. Klaus,[2] George Kollias,[3] Adriano Fontana,[4] Christopher R. Pryce,[2] Tobias Suter,[5] and Andrea Volterra[1,*]

[1]Department of Fundamental Neurosciences, University of Lausanne, Rue du Bugnon 9, 1005 Lausanne, Switzerland
[2]Department of Psychiatry, Psychotherapy and Psychosomatics, Psychiatric Hospital, University of Zurich, and Neuroscience Center Zurich, University of Zurich and ETH Zurich, August Forel-Str. 7, 8008 Zurich, Switzerland
[3]B.S.R.C. "Alexander Fleming", 34 Fleming Street, 16672 Vari, Greece
[4]Institute of Experimental Immunology Inflammation and Sickness Behaviour, University of Zurich, Winterthurerstr. 190, 8057 Zurich, Switzerland
[5]Neuroimmunology and MS Research, University Hospital Zurich, Sternwartestr. 14, 8091 Zurich, Switzerland
[6]Co-first author
[7]Present address: Department of Physiology, University of Bern, Bühlplatz 5, 3012 Bern, Switzerland
*Correspondence: andrea.volterra@unil.ch
http://dx.doi.org/10.1016/j.cell.2015.11.023

SUMMARY

The occurrence of cognitive disturbances upon CNS inflammation or infection has been correlated with increased levels of the cytokine tumor necrosis factor-α (TNFα). To date, however, no specific mechanism via which this cytokine could alter cognitive circuits has been demonstrated. Here, we show that local increase of TNFα in the hippocampal dentate gyrus activates astrocyte TNF receptor type 1 (TNFR1), which in turn triggers an astrocyte-neuron signaling cascade that results in persistent functional modification of hippocampal excitatory synapses. Astrocytic TNFR1 signaling is necessary for the hippocampal synaptic alteration and contextual learning-memory impairment observed in experimental autoimmune encephalitis (EAE), an animal model of multiple sclerosis (MS). This process may contribute to the pathogenesis of cognitive disturbances in MS, as well as in other CNS conditions accompanied by inflammatory states or infections.

INTRODUCTION

Synaptic activity is subject to various types of control, including regulatory inputs from surrounding glial cells. The release of gliotransmitters and factors from astrocytes induces synaptic modulation in cognitive circuits (reviewed in Araque et al. 2014) and could contribute to cognitive function (Halassa et al., 2009; Han et al., 2012; Lee et al., 2014; Suzuki et al., 2011). An astrocyte-synapse modulatory pathway was described in the hippocampal dentate gyrus (DG), by which synaptically activated astrocyte G-protein-coupled receptors (GPCR) stimulate, via glutamate release, NR2B-containing NMDA receptors located in presynaptic excitatory fibers (pre-NMDAR; Jourdain et al. 2007), resulting in the transient strengthening of entorhinal cortex (EC)-hippocampal DG excitatory synapses (Jourdain et al., 2007), a circuit implicated in contextual learning and memory (Denny et al., 2014; Liu et al., 2012). Surprisingly, the glial regulatory pathway is itself controlled by the cytokine tumor necrosis factor-α (TNFα) (Santello et al., 2011). Moreover, TNFα exerts additional controls at hippocampal synapses, such as on trafficking of AMPA (Beattie et al., 2002) and GABA_A receptors (Pribiag and Stellwagen, 2013), emerging as a key physiological regulator of hippocampal synaptic function. Therefore, it is important to ask what happens to the hippocampal cognitive circuit when TNFα increases above local homeostatic levels (Santello and Volterra, 2012), as occurs in the CNS in a variety of medical conditions linked to inflammation or infection (Clark et al., 2010).

Observations in both humans and animals indicate a link between increased TNFα levels and cognitive alterations (Swardfager and Black, 2013; Yirmiya and Goshen, 2011), but data are descriptive and no study to date has identified the specific mechanisms. Here, starting from the known characteristics of astrocytic modulation of DG synapses (Jourdain et al., 2007; Santello et al., 2011), and the specific observation that TNFα levels above a certain threshold (>300 pM) trigger glutamate release from astrocytes (Bezzi et al., 2001; Domercq et al., 2006; Santello et al., 2011), we asked whether such a condition can affect excitatory transmission at perforant path-granule cell (PP-GC) hippocampal synapses. We find that high (600 pM), but not low (60 pM), TNFα concentrations persistently alter the functional properties of this synaptic circuit, acting via TNF receptor type 1 (TNFR1) and a presynaptic mechanism involving NR2B-containing NMDAR. We also show that the same synaptic alteration, together with impaired contextual memory processing, is present in a murine model of multiple sclerosis (MS), a pathology often presenting with cognitive disturbances (Chiaravalloti and DeLuca, 2008). Finally, taking advantage of a transgenic mouse model, we directly demonstrate that both synaptic and cognitive impairments in the murine MS model depend to a large extent on activation of TNFR1 in astrocytes.

Cell

RESULTS

Increased TNFα Persistently Changes Excitatory Transmission in a Hippocampal Cognitive Circuit

To establish whether an increased local level of TNFα affects cognitive circuits, we initially compared the effect produced on excitatory EC-DG synapses by a rapid (10-s) puff of exogenous TNFα, applied at the estimated basal concentration (60 pM; Santello et al. 2011) or at a 10-fold higher concentration (600 pM; Figure 1). We used this experimental approach to evaluate the confined effect of the cytokine in the outer/middle molecular layer (OML/MML) of the DG (Figure 1A), and to directly link the observed effect to the used concentration. Application of 60 pM TNFα did not produce any detectable change in basal synaptic activity (mean frequency, amplitude, and kinetics of AMPAR-dependent miniature post-synaptic excitatory currents [mEPSCs]) in dentate GCs within 30 min (Figures 1A–1C and S1). In contrast, application of 600 pM TNFα produced progressive, strong increase in synaptic activity that reached plateau within 10 min and persisted unchanged after 30 min (and, in a few longer experiments, also after 50–60 min; data not shown). This long-lasting effect of the cytokine affected mEPSC frequency selectively, without changing mEPSC amplitude or kinetics (Figures 1A–1C and S1A), suggesting a presynaptic mechanism. When applied via prolonged bath incubation (1–2.5 hr), 600 pM TNFα, however, in addition to mEPSC frequency, also increased mEPSC amplitude, albeit slightly (Figure S1B), suggesting that its action at excitatory synapses is both dose and time dependent. These recordings were performed in young mice (P17–P25), but comparable effects were observed in adult animals (P60–P90; Figure 1D), ruling out that the TNFα effect is a developmental phenomenon. Increased mEPSC frequency in GCs predicts an enhanced EC drive to the DG. To verify this, we recorded EPSCs evoked by lateral PP stimulation (eEPSCs) in individual GCs (Figures 1E and 1F). Brief puffs of 600 pM TNFα, but not 60 pM, induced long-lasting increase in eEPSC amplitude and parallel change in short-term plasticity, denoted by reduced paired-pulse facilitation upon two consecutive stimuli. We conclude that high TNFα persistently enhances glutamate release probability at presynaptic PP terminals, thereby producing aberrant excitability of hippocampal GCs.

The TNFα Effect Requires Activation of TNFR1 and Ifenprodil-Sensitive NMDAR

Given that TNFα above 300 pM triggers glutamate release from astrocytes and that astrocytic glutamate transiently strengthens GC synapses via activation of NR2B-containing pre-NMDAR (Bezzi et al., 2001; Jourdain et al., 2007; Santello et al., 2011), we tested whether the long-lasting synaptic effect of elevated TNFα was sensitive to the NR2B antagonist, ifenprodil. Indeed, in the presence of this drug, 600 pM TNFα failed to change mEPSC frequency (Figure 2A). To then check whether TNFα activates NR2B-NMDAR persistently, we applied ifenprodil at the peak of the synaptic effect of the cytokine. The NMDAR antagonist was ineffective at reversing the TNFα increase in mEPSC frequency (Figure 2B). Therefore, the long-lasting synaptic action of TNFα necessitates NR2B-NMDAR activation, but only during its induction. Next, we hypothesized a role

for TNFR1, given that specific TNFR1 agonist antibodies mimic the glutamate-releasing action of TNFα in astrocytes (Bezzi et al., 2001). When we applied 600 pM TNFα to hippocampal slices from $tnfr1^{-/-}$ mice (Rothe et al., 1993), the cytokine failed to produce any increase in mEPSC frequency (Figure 2C), although basal activity at GC synapses was normal (mEPSC frequency: wild-type: 1.63 ± 0.23 Hz [n = 11]; $tnfr1^{-/-}$: 1.87 ± 0.28 [n = 4], p = 0.57; amplitude: wild-type: 7.91 ± 0.74 pA; $tnfr1^{-/-}$: 6.57 ± 0.57, p = 0.32, unpaired t test). Taken together, these data confirm that TNFR1 plays a necessary role in the synaptic effect of TNFα and suggest that, at increased levels, the cytokine stimulates astrocyte signaling via this receptor.

$tnfr1$ Knockout Mice Conditionally Re-expressing the Receptor in Astrocytes Selectively

To establish that elevated TNFα indeed affects synaptic function via astrocyte signaling, we generated a new double transgenic mouse model, the $hGFAPcreT2/tnfr1^{cneo/cneo}$ mouse. To obtain this model, we crossed mice with TNFR1 conditionally deleted in all cell types ($tnfr1^{cneo/cneo}$; Victoratos et al. 2006), which behave as functional $tnfr1$ knockout mice and lack any response to 600 pM TNFα at GC synapses (data not shown), with mice allowing TNFR1 re-expression selectively in astrocytes via tamoxifen (TAM)-inducible cre recombination driven by the human glial fibrillary acidic protein promoter ($hGFAPcreT2$; Hirrlinger et al. 2006), details in Figure 3A). The efficiency and specificity of astrocytic recombination in the hippocampal DG was determined using $hGFAPcreT2/tnfr1^{cneo/cneo}$ mice expressing the ROSA-EYFP reporter (Srinivas et al., 2001) (Figure 3B). Young (P22) and adult (P90) mice, studied 13 and 25 days after the first TAM injection, respectively, yielded similar results. In 12 slices from four P90 mice, we counted a total of 1,680 EYFP$^+$ cells, most of which displayed the typical morphology of protoplasmic astrocytes and were distributed patchily, both in the dentate molecular layer (ML) and in the hilus. These cells were also positive for the astrocytic marker glutamine synthetase (GS$^+$/EYFP$^+$ cells) and represented 37% of the total astrocytic population (GS$^+$ cells). About 10% of the EYFP$^+$ cells were confined to the subgranular zone (SGZ), most likely representing stem cells and neuronal precursors. In the OML/MML, where PP-GC synapses lie, 99.3% (714 cells) of the EYFP$^+$ cells were GS$^+$, representing resident astrocytes, while 0.7% (five cells) were NeuN$^+$ or GS$^-$, representing immature GCs sitting in the GC layer and sending growing dendrites to the OML/MML. No reporter expression was detected in mice injected with corn oil (OIL), the TAM vehicle (Figure S2), confirming that cre activity is specifically induced by TAM. The above results were corroborated by genomic PCR analysis of TAM-induced $tnfr1$ recombination in FACS-sorted populations of NeuN$^+$ cells (no recombination) and NeuN$^-$ cells (prominent recombination) obtained from $hGFAPcreT2/tnfr1^{cneo/cneo}$ mouse brains (Figures 3C, S3, and S4). Therefore, $hGFAPcreT2/tnfr1^{cneo/cneo}$ mice are a valid model to investigate the contribution of astrocyte signaling to the actions of TNFα.

Astrocyte-Selective TNFR1 Expression Largely Reconstitutes the Synaptic Effect of TNFα

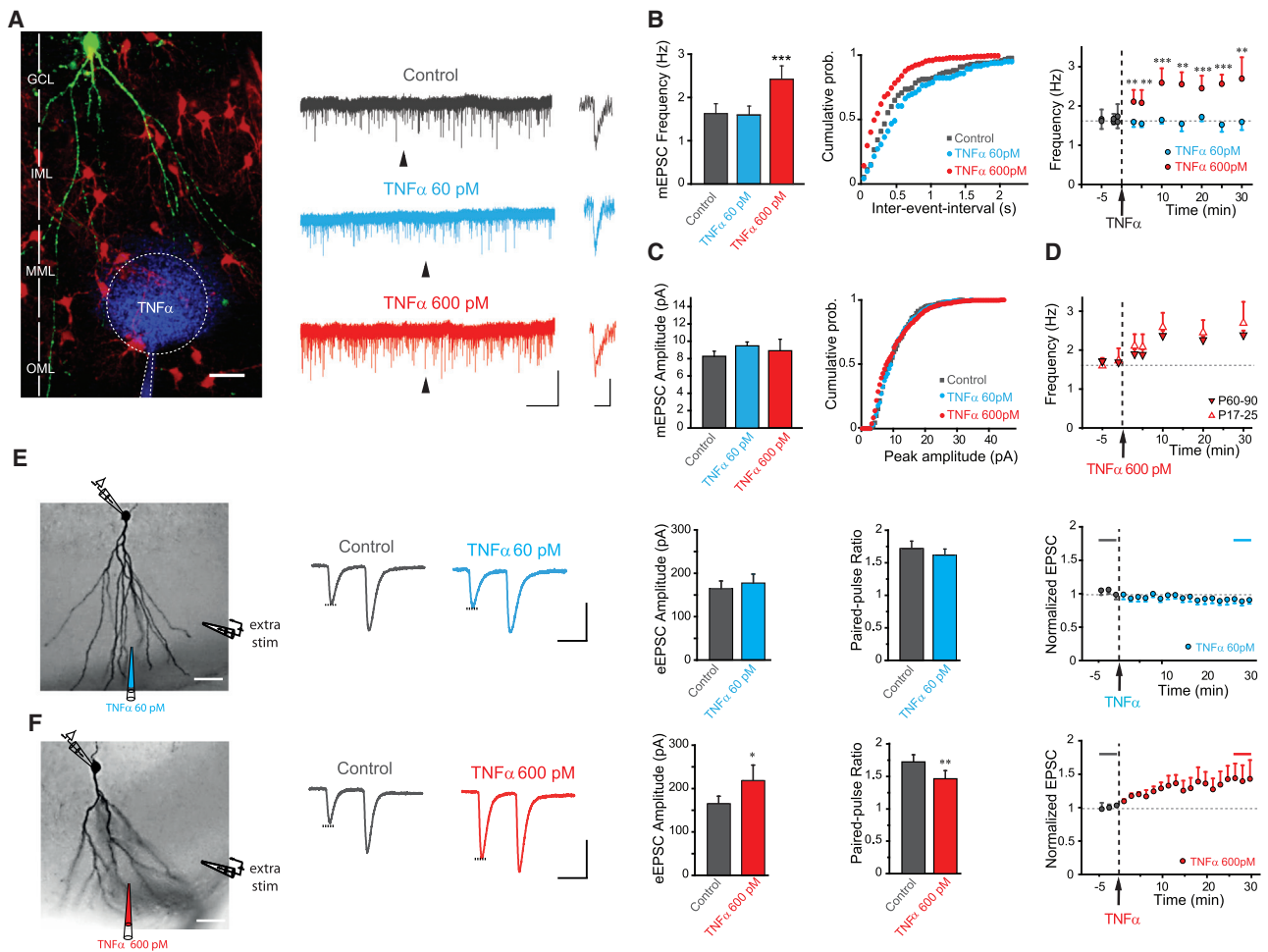Next, we investigated whether TNFα has an effect at PP-GC synapses in TAM-injected $hGFAPcreT2/tnfr1^{cneo/cneo}$ mice

Figure 1. Concentration-Dependent Effects of Exogenous TNFα on Excitatory Synaptic Activity in a Hippocampal Cognitive Circuit

(A) Left: two-photon image of the experimental setting for local TNFα application in the hippocampal DG (GC: green, Alexa-488; astrocytes: red, sulforhodamine 101; TNFα diffusion upon 10-s local puff: Cascade blue with dotted white contour). Scale bar, 20 μm; GCL, granule cell layer; IML, MML, and OML, inner, middle and outer molecular layer, respectively. Right: representative traces of mEPSC activity in control condition (gray) and 30 min after puffing 60 pM TNFα (azure) or 600 pM TNFα (red). Scale bars, 20 s, 20 pA. Insets: representative mEPSC events for each condition taken at the indicated time (triangle). Scale bars, 10 ms, 5 pA.

(B) Left: histograms of mean mEPSC frequency in control condition (n = 16) and 30 min after puffing 60 pM TNFα (n = 5) or 600 pM TNFα (n = 11). Only the latter treatment increases mEPSC frequency versus control (p < 0.001, ANOVA followed by post hoc comparisons: ANOVA + phc). Middle: representative cumulative probability plots comparing mEPSC inter-event intervals (IEI) in the above conditions. Right: mEPSC activity monitored from 5 min before puffing TNFα (puff denoted by arrow) to 30 min after puffing; azure: 60 pM TNFα; red: 600 pM TNFα. Only the latter increases mEPSC frequency (repeated-measures ANOVA + phc: at 3, 5, 15, and 30 min: p < 0.01; at 10, 20, and 25 min: p < 0.001).

(C) Histograms (left) and cumulative probability plots (right) of mean mEPSC amplitude before (control) and 30 min after application of 60 pM or 600 pM TNFα. Neither TNFα concentration produced an effect (p > 0.1, ANOVA).

(D) Comparison of the effect of 600 pM TNFα in young (n = 11) and adult (n = 14) mice. In both groups TNFα maximally increased mEPSC frequency within 10 min (p < 0.001; two-way repeated-measures ANOVA + phc) with comparable effect (p > 0.08).

(E) Left: biocytin staining of the recorded GC showing location of the stimulating electrode and of the puffing pipette containing 60 pM TNFα, accompanied by representative traces (average of six consecutive sweeps) showing paired EPSCs before and 30 min after TNFα puff. Scale bars, 40 ms; 200 pA. Middle: histograms of mean EPSC amplitude and paired-pulse ratio (PPR) in control condition and 30 min after puffing 60 pM TNFα (n = 5; p > 0.27 and p > 0.12, respectively). Right: time course of the effect of 60 pM TNFα on mean EPSC amplitude (normalized value).

(F) Left: GC biocytin staining and corresponding EPSC traces recorded before and after puffing 600 pM TNFα (conditions like in E, left). Scale bars, 40 ms; 200 pA. Middle: histograms represent mean eEPSC amplitude and PPR in control condition and 30 min after puffing 600 pM TNFα. The cytokine causes substantial increase of EPSC amplitude (n = 9; p < 0.05) and decrease in PPR (n = 9; p < 0.01). Right: time course of the effect of 600 pM TNFα on mean EPSC amplitude (normalized value). TNFα induces progressive and irreversible increase in synaptic activity. Data are presented as mean ± SEM.
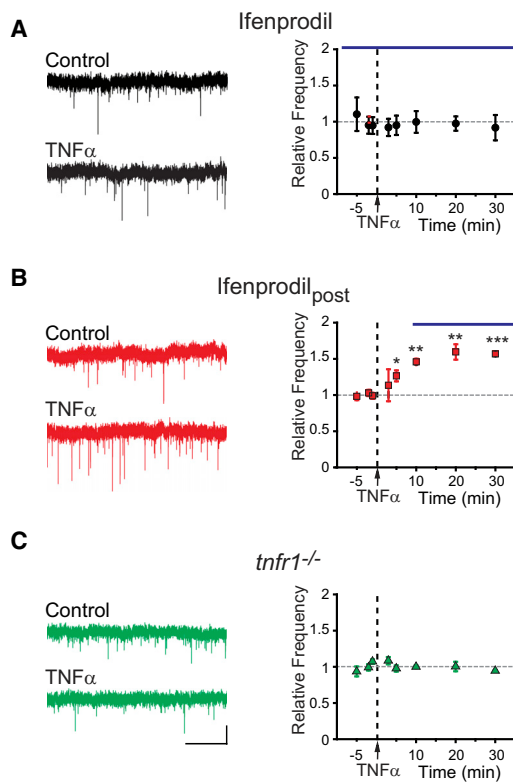
See also Figure S1.

Cell

Figure 2. The Mechanism of the Synaptic Change Induced by TNFα: The Role of Ifenprodil-Sensitive NMDA Receptors and of TNFR1

(A–C) Left: representative traces of mEPSC frequency in a GC before (control) and 30 min after puffing 600 pM TNFα (different conditions in A, B, and C specified below). Right: time course of the mean effect of TNFα (normalized value). Scale bars: 5 pA; 5 s. Statistics: repeated-measures ANOVA + phc. (A) TNFα effect in the presence of the NR2B-selective NMDAR antagonist ifenprodil (3 μM, blue bar). The cytokine does not change mEPSC frequency (n = 4, p > 0.5 at all time-points after TNFα versus before TNFα). (B) TNFα effect when ifenprodil is applied 10 min after puffing the cytokine (ifenprodil$_{post}$). Ifenprodil does not reverse the mEPSC frequency increase induced by TNFα (n = 4; p < 0.05: at 5 min post-TNFα; p < 0.01 at 10 and 20 min; p < 0.001: at 30 min versus before TNFα). (C) TNFα effect in $tnfr1^{-/-}$ mice. Lack of TNFR1 prevents the effect of TNFα (n = 4; p > 0.4 at all time points after TNFα versus before TNFα). Data are presented as mean ± SEM.

with TNFR1 expression functionally reconstituted selectively in astrocytes. Experiments were conducted 10–11 days after TAM onset. A puff of 600 pM TNFα locally in the MML/OML significantly increased mEPSC frequency in GCs (Figure 4A). The cytokine effect was slow and persistent, as observed in wild-type mice (Figure 1B), but less pronounced, possibly because only part of the astrocytic population re-expresses TNFR1 (Figure 3B). In contrast, application of TNFα to slices from OIL-injected *hGFAPcreT2/tnfr1$^{cneo/cneo}$* mice (global *tnfr1* knockouts, no TAM-induced recombination) produced no synaptic effect (Figure 4B). Any unspecific effect of TAM was also excluded, since in slices from TAM-injected *tnfr1$^{cneo/cneo}$* mice, in which TAM cannot induce recombination, TNFα did not affect mEPSC activity (Figure 4C). Therefore, expression of TNFR1 exclusively in GFAP-positive cells

faithfully reproduces the persistent effect of TNFα on mEPSC frequency observed in wild-type mice.

Cognitive Impairment, Local Inflammation, and Enhanced TNFα Levels in the Hippocampus of a Mouse Model of Multiple Sclerosis

Next, we evaluated whether the identified astrocytic cascade triggered by high TNFα and causing persistent alteration of a cognitive synaptic circuit, is activated in a defined pathological condition and contributes to cognitive pathogenesis. We focused on multiple sclerosis (MS) because (1) about 50% of MS patients suffer from cognitive disturbances (Chiaravalloti and DeLuca, 2008) and present anatomical/functional alterations in cognitive areas, including hippocampal DG (Gold et al., 2010), and (2) in both MS patients and animal models of the pathology, notably experimental autoimmune encephalomyelitis (EAE), TNFα/TNFR1 signaling is implicated in pathogenesis (Eugster et al., 1999; Gregory et al., 2012; Kassiotis and Kollias, 2001). Our studies were performed in the EAE mouse model, using an adoptive transfer induction protocol (AT-EAE; Codarri et al. 2011; see the Experimental Procedures), which allows the EAE CNS pathology to develop effectively also in TNFR1-deficient mice. We selected a cognitive test assessing functioning of the EC-DG circuitry, contextual fear conditioning (Anagnostaras et al., 2001; Denny et al., 2014; Liu et al., 2012) and investigated in adult C57BL/6J mice (P60–P90) the effects of AT-EAE in its early phase (days 6 and 7 after transfer of autoimmune T cells [6–7 dpi]), when classical EAE symptoms leading to ascending flaccid paralysis are absent (Figure S5). An initial activity test (AT) excluded any confounding motor or emotional deficits due to AT-EAE (Figure 5A). Moreover, lack of effect on locomotor activity, freezing, or rearing indicated that motor function, exploration, and normal anxiety state, respectively, were intact (Figure S6). Subsequently, the mice underwent fear conditioning. Both control (sham-treated) and AT-EAE mice learned proficiently and acquired conditioned fear across the session, with AT-EAE mice showing a trend to lower freezing (Figure 5A). The distance moved during electroshock was used as a measure of pain sensitivity, and there was no effect of AT-EAE (Figure S6). The next day we measured expression of long-term contextual memory. Only control mice exhibited the expected level of fear expression that they acquired on day 6. AT-EAE mice, in contrast, displayed a marked deficit in contextual memory (Figure 5A). To investigate if this deficit was associated with the presence of a local pathology, we next performed immunohistochemistry experiments using leukocyte and microglia markers in hippocampal tissue (Figure 5B). Compared to controls, AT-EAE mice (8–14 dpi) showed an accumulation of infiltrating leukocytes at the border between the third ventricle and DG and CA3 parenchyma. Moreover, within the parenchyma, microglia displayed the reactive phenotype, with enlarged cell bodies and shortened processes. The amount of reactive and/or infiltrating cells decreased progressively from the regions contacting the third ventricle to the more distal ones, like CA1 and CA2. For simplicity, we refer to this pathology as "local inflammation." We also measured TNFα protein levels in punches of hippocampal tissue obtained (8 dpi) from the same mice studied in the contextual memory test (Figure 5C). The local level of TNFα
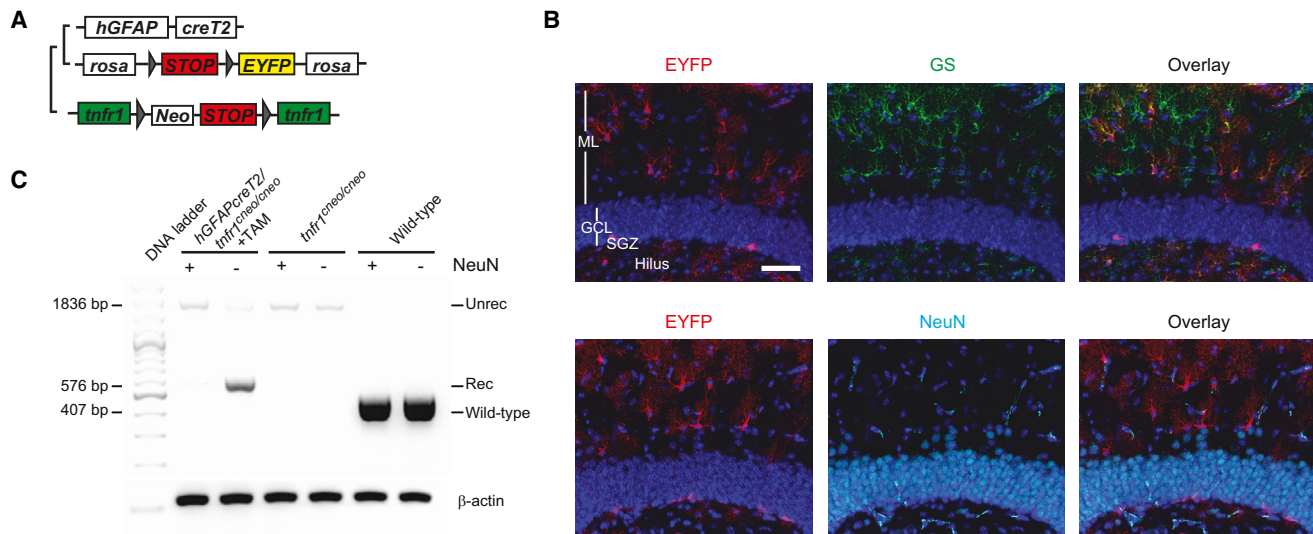
Figure 3. Characterization of *hGFAPcreT2/tnfr1*^{cneo/cneo} Mice, a Model of Conditional TNFR1 Knockout, in which TNFR1 Can Be Re-expressed Selectively in Astrocytes

(A) Scheme of the model: mice expressing TAM-inducible *cre* recombinase under the *hGFAP* promoter (*hGFAPcreT2*) and a conditional reporter (STOP-EYFP, gray triangles) in the *ROSA* locus are crossed with mice (*tnfr1*^{cneo/cneo}) with a neomycin cassette (Neo-STOP) flanked by loxP sites inserted in the *tnfr1* gene to conditionally inhibit its functional expression.

(B) Representative immunolabeling of the hippocampal DG of a P90 *hGFAPcreT2/tnfr1*^{cneo/cneo} mouse upon TAM-induced recombination (z stack, 12 μm; scale bar, 100 μm). Upper panels, left: reporter expression revealed by anti-EYFP antibodies (EYFP, red). Middle: astrocyte staining with glutamine synthetase (GS, green). Right: overlay showing co-localization of the reporter with astrocytes in the dentate ML and hilus. Notice few additional EYFP⁺ cells in the sub-granular zone (SGZ), representing neural stem cells and/or neuronal precursors. Blue: DAPI nuclear staining. Lower panels, left: reporter expression as above. Middle: neuronal staining with NeuN (turquoise). Right: overlay showing no co-localization of the reporter with neurons. (See also Figure S2 for immunolabeling of OIL-treated *hGFAPcreT2/tnfr1*^{cneo/cneo} mice.)

(C) Genomic PCR analysis of *tnfr1* expression in FACS-sorted neuronal (NeuN⁺) and non-neuronal (NeuN⁻) cell populations from the brains of TAM-injected *hGFAPcreT2/tnfr1*^{cneo/cneo}, *tnfr1*^{cneo/cneo}, and wild-type mice. The lower band (407 bp) corresponds to the wild-type *tnfr1* sequence; the upper one (Unrec, 1,836 bp) corresponds to the presence of the neo cassette in the *tnfr1* sequence (lack of *tnfr1* expression); and the intermediate band (Rec, 576 bp) corresponds to the removal of the neo cassette sequence between the 2 loxP sites upon recombination (*tnfr1* re-expression). Note the combined appearance of a strong Rec band and a reduced Unrec band selectively in the NeuN⁻ population from TAM-injected *hGFAPcreT2/tnfr1*^{cneo/cneo} mice. See also Figures S3 and S4. The *β-actin* promoter amplicon (bottom) shows the presence of similar amounts of DNA in the reactions. On the left: molecular weight marker: 100 bp DNA ladder. The gel was cut below 100 bp for aesthetic reasons.

See also Figures S2, S3, and S4.

was increased 8-fold in AT-EAE mice compared to controls. The increase was specific to dorsal hippocampus, the region bordering the third ventricle, which is integral to the contextual learning and memory circuitry (Anagnostaras et al., 2001). Therefore, at a stage of EAE that is fully asymptomatic in terms of motor pathology (8 dpi), mice present with overt local inflammatory pathology and enhanced TNFα levels in the hippocampus that could account for the observed contextual memory defect.

Altered Hippocampal Excitatory Transmission in AT-EAE: The Protective Effect of Ifenprodil

Next, we checked the state of the synaptic circuitry supporting contextual memory in AT-EAE mice (P60–P90, 8–14 dpi). The paired-pulse ratio of eEPSCs at PP-GC synapses was significantly reduced compared to controls, indicative of an increased glutamate release from PP terminals. Consistently, the synaptic input-output relationship was altered, with significantly greater eEPSC amplitudes evoked by the same stimulation intensity (Figure 6A). These defects strongly resemble those induced by high TNFα in younger mice (Figures 1E and

1F). In keeping, AT-EAE mice also displayed significantly higher mEPSC activity in GCs than controls (Figure 6B). The augmentation was most prominent in mEPSC frequency (34%), less pronounced in amplitude (16%), whereas kinetics were unchanged (rise time: p = 0.19; decay time: p = 0.47, [n = 16] unpaired t test). Given that ifenprodil prevents the increase in mEPSC frequency induced by TNFα in young mice (Figure 2A), we tested whether the drug was effective also in adult AT-EAE mice. In mice treated with ifenprodil in vivo during AT-EAE induction (see details in the Supplemental Experimental Procedures), mEPSC frequency in GCs was lower than in untreated AT-EAE mice, and comparable to that in controls (Figure 6C). However, when ifenprodil was applied acutely to slices from untreated AT-EAE mice, the drug failed to decrease mEPSC frequency (before ifenprodil: 2.51 ± 0.16 Hz; after ifenprodil: 2.16 ± 0.18 Hz; n = 8; p = 0.09, paired t test). These data suggest that NR2B-containing NMDAR participate in the induction (but not maintenance) of the persistent change of PP-GC excitatory transmission induced by AT-EAE. Intriguingly, the in vivo treatment with ifenprodil did not counteract the mEPSC
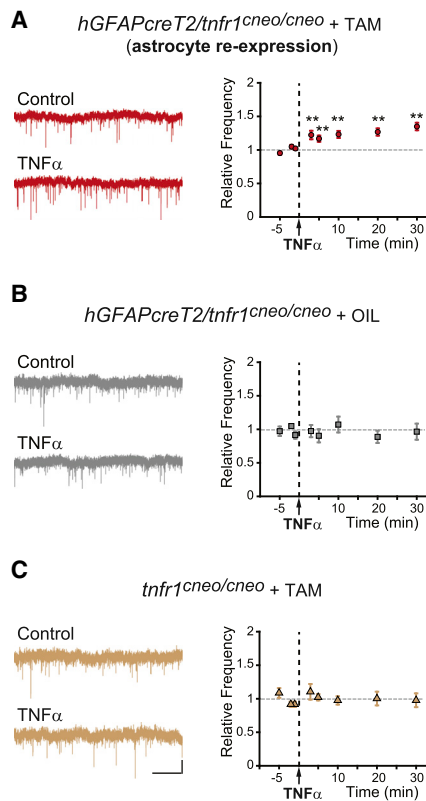
Cell

Figure 4. Re-expression of TNFR1 Selectively in Astrocytes Reconstitutes the Synaptic Effect of TNFα

(A–C) Left: representative traces of mEPSC frequency in a GC before (control) and 30 min after puffing 600 pM TNFα (different conditions in A, B, and C specified below). Right: time course of the mean effect of TNFα (normalized value). Scale bars, 5 pA, 5 s. Statistics: repeated-measures ANOVA + phc. (A) TNFα effect in TAM-injected $hGFAPcreT2/tnfr1^{cneo/cneo}$ mice. The cytokine induces a persistent increase in mEPSC frequency (n = 7; p < 0.01 at all time points after TNFα versus before TNFα). (B) TNFα effect in OIL-injected $hGFAPcreT2/tnfr1^{cneo/cneo}$ mice. Without TAM-induced recombination, TNFα does not change mEPSC frequency (n = 3; p > 0.3 at all time-points after TNFα versus before TNFα). (C) TNFα effect in TAM-injected $tnfr1^{cneo/cneo}$ mice. With TAM, but without *cre* activity, TNFα does not change mEPSC frequency (n = 5; p > 0.2 at all time points after TNFα versus before TNFα). Data are presented as mean ± SEM.

amplitude increase observed in AT-EAE mice (Figure 6C), suggesting that this component of the synaptic change is NR2B-independent.

A Causal Role of Astrocyte TNFR1 Signaling in the Hippocampal Synaptic Alterations and Cognitive Impairment Induced by AT-EAE

To determine whether the synaptic changes observed in AT-EAE mice depend on TNFα acting via astrocyte TNFR1 signaling, we next induced AT-EAE in TAM- or OIL-treated adult $hGFAPcreT2/tnfr1^{cneo/cneo}$ mice (see the Experimental Procedures for temporal details). mEPSC frequency in GCs of TAM-treated AT-EAE mice (astrocyte TNFR1 re-expression) was significantly higher than in their OIL-treated counterparts

(Figure 7A) and similar to that seen in wild-type AT-EAE mice (Figure 7B; p = 0.1, unpaired t test). mEPSC amplitude did not differ, however, from that of wild-type AT-EAE mice (p = 0.14, ANOVA followed by post hoc comparisons). The effect on mEPSC frequency was not due to TAM per se, because TAM-treated AT-EAE $tnfr1^{cneo/cneo}$ mice (no recombination) did not show any increased mEPSC frequency (Figure 7B). All four transgenic groups developed a similar pattern of local inflammation in the hippocampal DG, apparently indistinguishable from that seen in wild-type AT-EAE mice (compare Figures 5B and 7C), indicating that the TNFR1-dependent synaptic changes are triggered downstream of the local inflammatory reaction. To investigate whether astrocyte TNFR1 signaling is also responsible for impaired contextual memory in AT-EAE mice, we studied three groups of AT-EAE mice: TAM- or OIL-treated $hGFAPcreT2/tnfr1^{cneo/cneo}$ and TAM-treated $tnfr1^{cneo/cneo}$. At 5 dpi, mice were given an open-field test that excluded any group difference in behaviors relevant to motor function, anxiety, and exploration (Figure S7). At 6 dpi, contextual fear conditioning was conducted. All three groups demonstrated acquisition of freezing (Figure 7D), with OIL-treated $hGFAPcreT2/tnfr1^{cneo/cneo}$ mice and TAM-treated $tnfr1^{cneo/cneo}$ mice exhibiting a similar amount of conditioning, consistent with the absence of any TAM effect. TAM-treated $hGFAPcreT2/tnfr1^{cneo/cneo}$ mice exhibited proportionally less acquisition of freezing relative to the other two groups. This deficit was not due to reduced sensitivity to the electroshock because all groups moved the same distance during electroshock (Figure S7). At 7 dpi, mice were tested for fear expression. TAM-treated $hGFAPcreT2/tnfr1^{cneo/cneo}$ mice showed a trend to decreased freezing relative to the other two groups (Figure 7D, middle), which was proportional to the decreased fear acquisition of the previous day. At 8 dpi, in a second fear expression test, TAM-treated $hGFAPcreT2/tnfr1^{cneo/cneo}$ mice exhibited further reduction of fear expression and significantly less expression than the two other groups (Figure 7D, right). These data indicate a cognitive phenotype in TAM-treated $hGFAPcreT2/tnfr1^{cneo/cneo}$ mice similar to that observed in wild-type AT-EAE mice. The latter presented, however, lower initial learning deficit and faster-onset memory deficit, differences that could be due to intrinsic variability of the AT-EAE protocol across experiments. We exclude other confounding factors because a second open-field test conducted at 9 dpi confirmed lack of locomotor and exploratory behavioral differences between groups (data not shown). We conclude that astrocyte TNFR1 expression is required for both functional alteration of the EC-DG synaptic circuit and contextual learning and memory deficit in AT-EAE mice.

DISCUSSION

Our study links a local increase in TNFα in the hippocampus to synaptic and cognitive dysfunction via astrocyte signaling. This astrocytic pathway is activated in EAE, an animal model of multiple sclerosis, and is necessary for the development of the contextual memory deficit observed and thus its delineation may reveal new therapeutic targets against cognitive decline (discussed below).
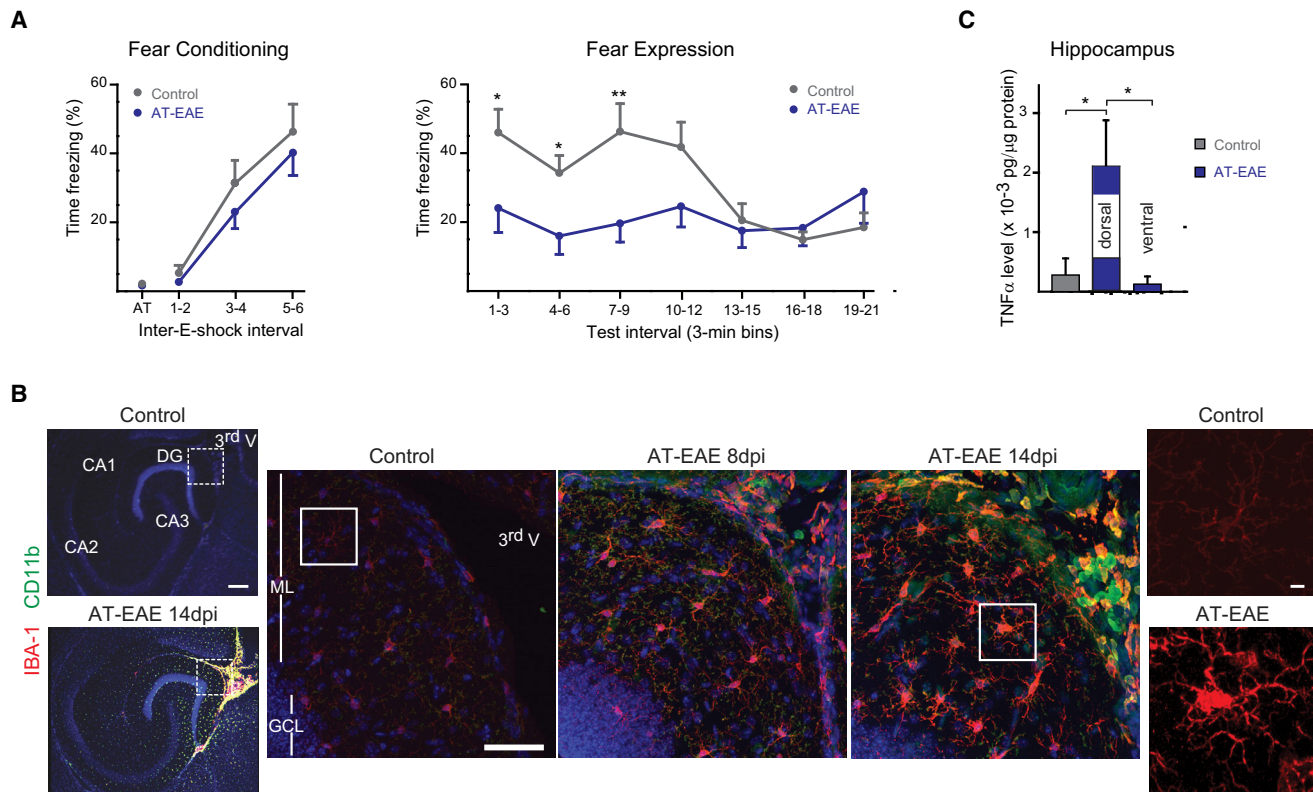
Figure 5. Impaired Cognitive Function, Local Inflammation, and Enhanced TNFα Levels in the Hippocampus of AT-EAE Mice

(A) Contextual fear learning and memory test in AT-EAE mice (6–7 dpi; blue, n = 7; see also Figures S5 and S6) versus vehicle-injected control mice (gray, n = 7). Left: acquisition of contextual fear conditioning. Mice were first exposed to an activity test (AT) and then to contextual fear conditioning (see also Figure S6). The two groups displayed a similar increase in the percent time spent freezing across intervals (interval main effect p < 0.001 ANOVA + phc) with AT-EAE mice showing slightly lower values. Right: expression of fear conditioning. AT-EAE mice exhibited decreased freezing (reduced fear memory) compared to control mice (group x interval interaction p < 0.001 ANOVA + phc) at intervals 1–3, 4–6, and 7–9 (p < 0.01, 0.05, and 0.001, respectively). In control mice, the level of freezing at the onset of the expression test was equivalent to that at the end of acquisition.

(B) Representative labeling of microglia and leukocyte markers (red, Iba1; green, CD11b) in the hippocampus at the border with the third ventricle (3rd V) in control condition and after AT-EAE induction; blue, DAPI nuclear staining. Left: large field view (scale bar, 500 μm). Notice in AT-EAE mice (14 dpi) a strong accumulation of CD11b- and/or Iba1-positive cells in the 3rd V and surrounding regions (DG and CA3), dissipating toward more distal regions (CA1 and CA2). Middle: enlarged views of the DG (ML, GCL) at the border with the 3rd V corresponding to the dotted squares on the left. The three panels compare the situation in control mice and in AT-EAE mice at 8 and 14 dpi (z stack, 45 μm; scale bar, 50 μm). An increasing number of infiltrating leukocytes (CD11b+) and activated microglia (Iba1+ and CD11b+) are seen with progression of AT-EAE pathology. Right: enlarged views (scale bar, 5 μm) of the white frames in the middle panels highlight the state change of microglia, from resting in control mice (faint Iba1 staining) to activated in AT-EAE mice (14 dpi; strong Iba1 staining);

(C) TNFα levels in the hippocampus of control (n = 7) and AT-EAE mice (8 dpi; n = 7; same mice as in A). Histograms show a significant increase in AT-EAE mice compared to controls, specifically in dorsal versus ventral hippocampus (p < 0.05; ANOVA + phc). In controls, TNFα values in dorsal and ventral hippocampus were analogous and grouped together. Data are presented as mean ± SEM.

See also Figures S5 and S6.

Astrocyte TNFR1 Is Required for Induction of Synaptic and Cognitive Defects

In EAE, activated microglia and infiltrating macrophages controlled by CD4+ T cells are the most likely cause of local TNFα increase in the DG (Figure 5B; Renno et al. 1995), whereas downstream activation of TNFR1 in astrocytes appears to be the critical event for induction of the core synaptic and behavioral phenotype. This is demonstrated by reconstitution of the phenotype in *hGFAPcreT2/tnfr1^cneo/cneo* mice, functional *tnfr1* knockouts in which TNFR1, via TAM-induced *cre* recombination, is re-expressed exclusively in GFAP-positive cells. Astrocytes represent the only population of such cells that we observed at

the time of our experiments (10–22 days from the start of recombination) in the dentate OML/MML, where excitatory PP-GC synapses are located. Recombination in the DG occurs also in the much smaller population of SGZ neural stem cells, but expression of TNFR1 in these cells and in the derived neuronal precursors and immature GCs very unlikely contributes to the TNFα-dependent phenotype because (1) different from astrocytes, these cells lie distally from PP-GC synapses (25 days after the start of recombination, those with growing dendrites able to reach the OML/MML were 0.7% of the resident recombined astrocytic population) and (2) full integration of newborn GCs into the excitatory network as mature GCs requires 8 weeks
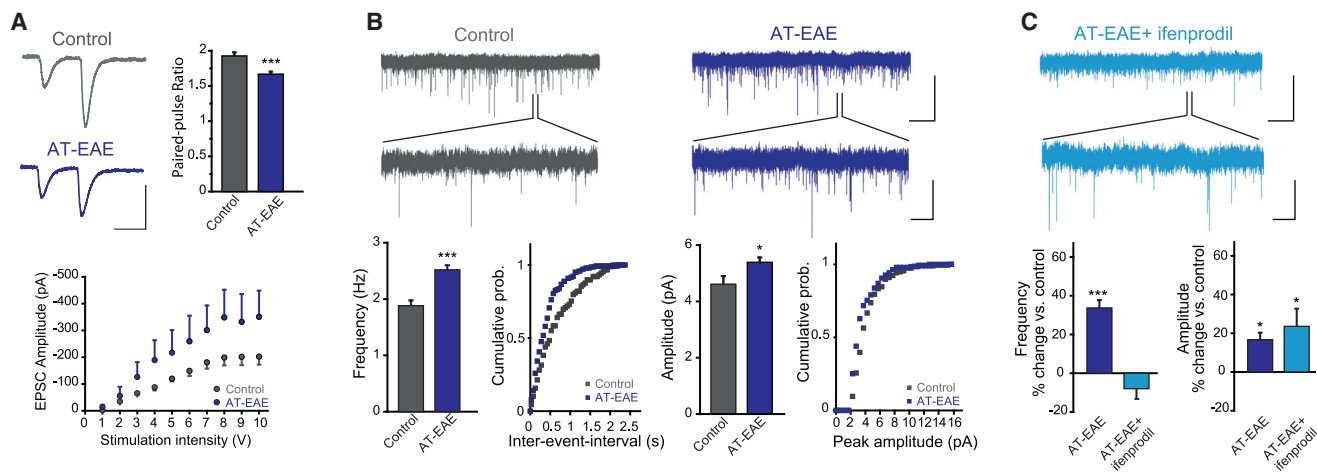
Cell

Figure 6. Altered Hippocampal Excitatory Transmission in AT-EAE: The Protective Effect of Ifenprodil

(A) Top: representative traces of evoked paired-pulse EPSCs in GCs from wild-type vehicle-treated (control, gray) and AT-EAE mice (9 dpi, blue). Scale bars, 40 ms; 200 pA. Stimulation was adjusted to obtain comparable initial EPSC amplitudes in the two groups. Short-term plasticity is altered in AT-EAE mice, leading to reduced paired-pulse facilitation. Histograms show mean PPR in the two conditions (control: n = 10; AT-EAE: n = 8; p < 0.001, unpaired t test). Bottom: mean amplitudes of single EPSCs plotted as function of the stimulus intensity. EPSCs are larger in GCs from AT-EAE mice than in GCs from control mice (n = 6 and 9, respectively; p < 0.05, two-way ANOVA + phc).

(B) Top: representative traces of mEPSC activity in dentate GCs from control (n = 16) and AT-EAE mice (12 dpi, n = 24). Scale bars, 20 s; 20 pA. The enlarged regions highlight an increased activity in AT-EAE mice. Scale bars, 2 s; 10 pA. Bottom: histograms and representative cumulative probability plots of mean mEPSC frequency (left) and amplitude (right) in control mice and in AT-EAE mice. Both parameters are significantly enhanced in AT-EAE mice (p < 0.001 and p < 0.05, respectively, unpaired t test).

(C) Top: representative trace of mEPSC activity in dentate GCs from AT-EAE mice treated with ifenprodil in vivo (azure, n = 14). Scale bars, 20 s; 20 pA. The enlarged region shows that activity is lower compared to untreated AT-EAE mice and similar to controls. Scale bars, 2 s; 10 pA. Bottom: histograms show the percent change in mean mEPSC frequency (left) and amplitude (right) versus control in AT-EAE mice treated (azure) or not (blue) with ifenprodil in vivo. Untreated, but not ifenprodil-treated, AT-EAE mice display higher mEPSC frequency than controls (p < 0.001 and p = 0.28, respectively, ANOVA + phc). Concerning mEPSC amplitude, both ifenprodil-treated and untreated AT-EAE mice display higher amplitude than controls (p < 0.05, ANOVA + phc). Data are presented as mean ± SEM.

(Toni et al., 2007), and in any case these cells may contribute to contextual memory formation only after 4 weeks of maturation (Gu et al., 2012), a time frame incompatible with the timing of our experiments.

Pathological TNFα Contributes to the Synaptic Alterations: The Signaling Mechanism

TNFα produces a persistent change in excitatory transmission only when its concentration increases up to levels that are specific to pathological states. In the early phases of AT-EAE, we measured an 8-fold increase in tissue TNFα levels in the dorsal hippocampus. This increase resembles in proportion the 10-fold increase that we used to mimic pathological (600 pM) versus physiological (60 pM) TNFα levels when applying the exogenous cytokine locally in the DG. In absolute value, 600 pM could represent a concentration close to the one reached by the cytokine during EAE, because at this concentration exogenous TNFα produced synaptic changes very similar, in both quality and quantity, to those observed in AT-EAE mice. While this value is much higher than the tissue concentration that we measured, it could mimic the TNFα concentration sensed by astrocytes locally, which may be orders of magnitude higher than the average concentration in the tissue (Wang et al., 2011). Regardless, 600 pM exogenous TNFα and the endogenous cascade operating in AT-EAE appear to act via the same mechanism,

as both enhance mEPSC frequency via astrocyte TNFR1 and an ifenprodil-sensitive mechanism. The latter data strongly suggests that TNFα activates at PP-GC synapses the same pathway triggered by astrocyte GPRC agonists in physiological conditions, ultimately resulting in stimulation of NR2B-containing pre-NMDAR (Jourdain et al., 2007; Santello et al., 2011), although the TNFα-induced activation must be different because it leads to long-lasting and irreversible modifications of synaptic activity. TNFα (upon prolonged incubation in normal mice) and the endogenous cascade of AT-EAE produce another common effect, a small increase in mEPSC amplitude. This effect is ifenprodil-insensitive and therefore mechanistically different from the astrocyte-mediated effect, which is clearly presynaptic. It could be, in contrast, post-synaptic, consistent with the reported capacity of TNFα to promote surface insertion of AMPAR subunits at dendritic spines via stimulation of neuronal TNFR1 (Stellwagen et al., 2005). The contribution of this latter mechanism to the synaptic and cognitive phenotype in AT-EAE remains to be defined given the substantial restoration of the phenotype upon TNFR1 re-expression selectively in astrocytes.

Local Malfunction of the Entorhinal Cortex-Hippocampal Excitatory Circuit

The TNFα/TNFR1-dependent synaptic changes identified here lead to alteration of the input-output relationship in the EC-DG
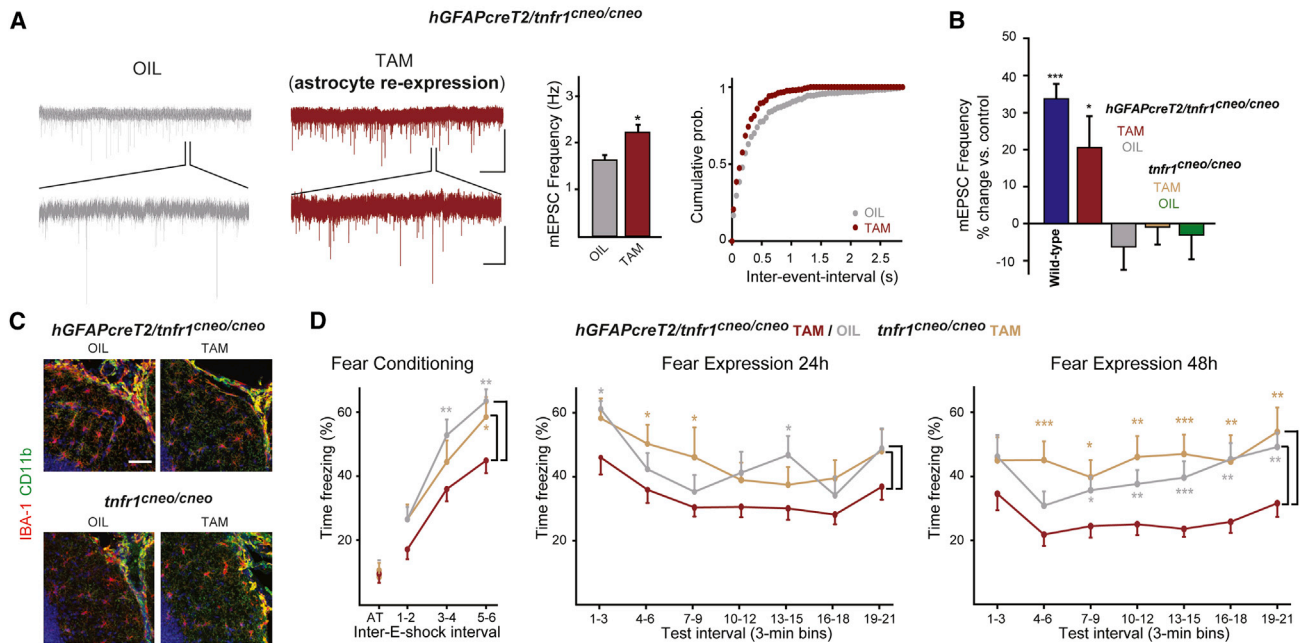
AT-EAE

Figure 7. A Causal Role of Astrocyte TNFR1 Signaling in the Hippocampal Synaptic Alterations and Cognitive Impairment Induced by AT-EAE

(A) Left: representative traces of mEPSC activity in dentate GCs upon induction of AT-EAE in mice re-expressing TNFR1 selectively in astrocytes (TAM-treated *hGFAPcreT2/tnfr1*^cneo/cneo^, dark red; n = 21) and in their direct controls (OIL-treated *hGFAPcreT2/tnfr1*^cneo/cneo^, gray; n = 11). Scale bars, 20 s; 20 pA. The enlarged regions highlight higher mEPSC activity in TAM-treated mice compared to OIL-treated ones. Scale bars, 2 s; 10 pA. Middle: histograms showing that mean mEPSC frequency is significantly higher in TAM-treated versus OIL-treated *hGFAPcreT2/tnfr1*^cneo/cneo^ AT-EAE mice (p < 0.05, unpaired t test). Right: representative cumulative probability plots comparing mEPSC IEI in the two above groups.

(B) Histograms showing comparative changes in mEPSC frequency in GCs induced by AT-EAE in several groups of mice with respect to wild-type controls. AT-EAE groups are wild-type mice (blue, n = 16), TAM- (dark red, n = 21) and OIL-treated (gray, n = 11) *hGFAPcreT2/tnfr1*^cneo/cneo^ mice, and TAM- (gold, n = 15) and OIL-treated (green, n = 19) *tnfr1*^cneo/cneo^ mice. AT-EAE causes an mEPSC frequency increase only in wild-type and TAM-treated *hGFAPcreT2/tnfr1*^cneo/cneo^ mice (p < 0.001 and p < 0.05 versus wild-type controls, respectively; ANOVA + phc). The latter two groups are not statistically different (p = 0.095, ANOVA).

(C) Representative labeling of microglia and leukocyte markers (Iba1, red; CD11b, green) in the hippocampal DG of TAM- or OIL-treated *hGFAPcreT2/tnfr1*^cneo/cneo^ (top) and *tnfr1*^cneo/cneo^ (bottom) AT-EAE mice. The pattern of local leukocyte infiltration and microglia activation is similar in the four groups of mice and resembles the one observed in wild-type AT-EAE mice (see Figure 5B); z stack, 20 μm; scale bar, 50 μm.

(D) Contextual fear learning and memory test in TAM-treated *hGFAPcreT2/tnfr1*^cneo/cneo^ (dark red, n = 21), OIL-treated *hGFAPcreT2/tnfr1*^cneo/cneo^ (gray, n = 12), and TAM-treated *tnfr1*^cneo/cneo^ mice (gold, n = 11) developing AT-EAE (6–8 dpi). Left: mice were first exposed to an activity test (AT) and then to contextual fear conditioning (see also open field data; Figure S7). For acquisition of fear conditioning, all groups displayed an increased percent time spent freezing (interval main effect p < 0. 001, ANOVA + phc). However, TAM-treated *hGFAPcreT2/tnfr1*^cneo/cneo^ mice acquired less fear conditioning than did their OIL-injected counterparts and TAM-treated *tnfr1*^cneo/cneo^ mice (group x interval interaction p < 0.003 ANOVA + phc), whereas the latter two groups were not different. Middle: fear expression test 24 hr later: there was no difference among the three groups although TAM-treated *hGFAPcreT2/tnfr1*^cneo/cneo^ mice showed a trend to reduced freezing (group main effect p = 0.06 ANOVA). Right: repetition of the fear expression test the next day (48 hr after conditioning). TAM-treated *hGFAPcreT2/tnfr1*^cneo/cneo^ mice showed a further decrease in freezing and exhibited decreased freezing compared to the other two groups (group main effect p < 0.002 ANOVA + phc), whereas OIL-treated *hGFAPcreT2/tnfr1*^cneo/cneo^ mice and TAM-treated *tnfr1*^cneo/cneo^ mice exhibited a similar percent time freezing. Asterisks are color-coded and refer to comparison with TAM-treated *hGFAPcreT2/tnfr1*^cneo/cneo^ mice. Data are presented as mean ± SEM.

See also Figure S7.

circuit, which is critically involved in contextual memory processing (Liu et al., 2012; Denny et al., 2014). Accordingly, we find altered contextual learning and memory performance in AT-EAE mice with increased TNFα levels in dorsal hippocampus. A persistently increased excitatory drive may reduce the dynamic range and impair long-term potentiation (LTP) (Goussakov et al., 2000; Pascual et al., 2005), a defect already observed in the DG with TNFα concentrations similar to those used in this study (Cunningham et al., 1996), and likely to cause abnormal processing of learning and memory-related information (Chapman et al., 1999; Tombaugh et al., 2002). Definitive proof of the causative role played by the observed synaptic alterations could be achieved by reducing the abnormal excitatory PP input to GCs in AT-EAE mice in vivo, e.g., optogenetically, and showing consequent amelioration of the cognitive deficit. This deficit appears to be in temporal overlap with a local inflammation pathology restricted to the hippocampal areas surrounding the third ventricle, notably the DG (Figure 5B, large

Cell

field). This suggests that the cognitive phenotype is locally generated and not due to a generalized inflammatory state of the brain, although it does not exclude other sites of local inflammation in other brain regions at these stages of the pathology (Haji et al., 2012), nor that other behavioral processes, e.g., auditory fear, might be impacted (Acharjee et al., 2013). Putting all the above data together, we propose that a causal chain links EAE local inflammation to synaptic alteration and cognitive dysfunction via the action of TNFα and its astrocyte TNFR1. In this context, our data bring together a number of sparse recent observations suggesting that TNFα is involved in the synaptic alterations observed in EAE and other CNS pathology models (Centonze et al., 2009; Haji et al., 2012; Xu et al., 2010; Yang et al., 2013) and that enhanced TNFα levels are associated with the manifestation of cognitive defects (Belarbi et al., 2012; Gabbita et al., 2012; Terrando et al., 2010; reviewed in Clark et al., 2010; Swardfager and Black 2013; but see Han et al., 2013).

Relevance for Cognitive Dysfunction in MS and Other Medical Conditions

While cognitive disturbances involving hippocampal alterations (Gold et al., 2010) affect a large number of MS patients (Chiaravalloti and DeLuca, 2008), the responsible mechanisms have remained elusive. The present findings provide a plausible mechanistic basis and also suggest that the mechanism responsible for cognitive dysfunction is distinct from the one causing the motor symptoms. In addition to MS, our findings may be relevant to other CNS pathologies characterized by cognitive disturbances and elevated gray matter TNFα levels, notably Alzheimer's disease (AD; McAlpine and Tansey, 2008). Indeed, in animal models of AD, TNFα signaling via TNFR1 has been implicated in learning and memory deficits (He et al., 2007). Other inflammatory states due to bacterial or viral infections directly affecting the CNS, and even peripheral inflammatory states that result in septic encephalopathy, are accompanied by cognitive disturbances (Clark et al., 2010; Swardfager and Black, 2013). They could therefore present synaptic alterations similar to those recognized in AT-EAE mice, caused by the identified astrocytic pathway. In view of these considerations, therapeutic agents targeting the described signaling steps, specifically astrocytic TNFR1 and pre-NMDAR, could be tested against cognitive disturbances in the above medical conditions. TNFR1 has been strongly implicated in the pathogenesis of MS (Gregory et al., 2012) and EAE (Kassiotis and Kollias, 2001), but not yet in the cognitive aspects. According to animal studies and recent clinical trials, selective blockade of TNFR1 function represents a promising therapeutic strategy in MS (Van Hauwermeiren et al., 2011). Development of TNFR1 antagonists with central action could offer the important additional advantage of tackling the cognitive component of the pathology. As for pre-NMDAR, at hippocampal synapses these receptors contain the NR2B subunit (Jourdain et al., 2007). NR2B antagonists are currently under clinical investigation in several neurologic and psychiatric disorders (Paoletti et al., 2013). For effective use against cognitive impairment in MS and other conditions, more selective "presynaptic NR2B agents" or agents acting on other subunits

typical of pre-NMDAR (Larsen et al., 2011) should, however, be developed.

EXPERIMENTAL PROCEDURES

Animal Models

All in vivo and ex vivo procedures were conducted under license and according to regulations of the Cantonal Veterinary Offices of Vaud and Zurich (Switzerland). $tnfr1^{-/-}$ mice (http://www.informatics.jax.org/allele/key/2493) (Rothe et al., 1993), $tnfr1^{cneo/cneo}$ mice (http://www.informatics.jax.org/allele/MGI:3686874) (Victoratos et al., 2006), and hGFAPcreT2 mice (http://www.informatics.jax.org/allele/MGI:4418665) (Hirrlinger et al., 2006) expressing a conditional EYFP reporter in the ROSA locus (www.informatics.jax.org/allele/key/22442) (Srinivas et al., 2001), all on C57BL/6 background, were generated and maintained as described in the original studies. The latter two lines were cross-bred to generate $hGFAPcreT2/tnfr1^{cneo/cneo}$ mice. To achieve gene recombination, $hGFAPcreT2/tnfr1^{cneo/cneo}$ and $tnfr1^{cneo/cneo}$ mice were administered TAM (100 mg/kg) dissolved in corn oil (OIL), or OIL alone as a control carrier, once per day for 8 consecutive days (Hirrlinger et al., 2006). For AT-EAE induction, mice were injected with effector MOG35-55-specific CD4+ T cells generated from 2D2 mice (details in Codarri et al. 2011). Intervals from the first TAM or OIL injection were 10–12 days in electrophysiology experiments without AT-EAE induction, 16–22 days if AT-EAE was induced, 13–16 days in behavior experiments in AT-EAE mice, 13 (young mice) and 25 days (adult mice) in immunohistochemistry experiments looking at EYFP reporter expression, and 16–22 days in the same experiments looking at inflammation markers.

Electrophysiology Experiments

Patch-clamp recordings were performed in acute brain horizontal slices at excitatory PP-GC synapses in the hippocampal DG. GCs were patched with borosilicate glass pipettes (3–5 MΩ) and voltage-clamped at –65 mV. All experiments were carried out at 34°C in the presence of picrotoxin (100 μM), to block GABA$_A$ receptor-mediated currents. To study mEPSC activity in isolation, tetrodotoxin (TTX, 1 μM) was added to block action potentials. To test the effect of TNFα (60–600 pM), the cytokine was locally applied via an ejection pipette positioned in the OML by using a single 10-s pulse (4–7 psi) delivered by a PV830 Pneumatic PicoPump (WPI). In some experiments we indirectly verified spatial diffusion and rapid washout of TNFα by co-ejecting Cascade blue, a fluorescent dye, under two-photon imaging. Recordings in each GC started about 10 min after reaching whole-cell and covered a period from 5 min before to 30 min after TNFα application. Stimulation of the PP was done with a theta electrode placed in the OML. Recordings were analyzed essentially as described in Jourdain et al. (2007) and Santello et al. (2011).

Immunohistochemistry

For immunofluorescence staining, 50-μm-thick horizontal slices were prepared from fixed brains by use of a cryo-microtome (Microm International). After permeabilization, slices were incubated with primary antibodies (72 hr, 4°C), then with secondary antibodies in 0.3% Triton X-100/PBS (2 hr, room temperature), and with DAPI (300 nM) to label nuclei. Large-field images in the hippocampus and neighboring regions were acquired using a Leica MZ16FA stereomicroscope (Leica Microsystems) equipped with Leica EL6000 illumination. In all other cases, images were acquired with a Leica SP5 AOBS confocal microscope (Leica Microsystems), using a 40× oil-immersion "HCX PL APO" objective (NA: 1.25–0.75). Analysis was done with ImageJ software (NIH).

Behavioral Experiments

Acquisition of contextual fear conditioning followed 24 hr later by a test of its expression (sometimes repeated at 48 hr) were used as tests of, respectively, contextual learning and memory. The fear conditioning test, in some cases preceded by an open-field test the day before, was carried out using a fear conditioning arena (context) with a grid floor that could be electrified; the arena was placed within an isolation chamber (Ugo Basile) and controlled by Ethovision XT software (Noldus). Mice were first given a 5-min activity test (AT)

without electroshocks to assess locomotor activity, baseline freezing, and rearing. Next, the conditioning session comprised six inescapable electroshocks (0.20 mA × 2 s each), delivered at 2-min intervals. After this test, mice were returned to their home cages until the following day, when they were placed back in the same arena in the absence of electroshocks for the mnemonic fear expression test. Mice were considered to be freezing if no movement was detected for at least 2 s and the measure was expressed as a percentage of time spent freezing.

A detailed description of all experimental methods is provided in the Supplemental Experimental Procedures.

SUPPLEMENTAL INFORMATION

Supplemental Information includes Supplemental Experimental Procedures and seven figures and can be found with this article online at http://dx.doi.org/10.1016/j.cell.2015.11.023.

AUTHOR CONTRIBUTIONS

ACKNOWLEDGMENTS

REFERENCES

Acharjee, S., Nayani, N., Tsutsui, M., Hill, M.N., Ousman, S.S., and Pittman, Q.J. (2013). Altered cognitive-emotional behavior in early experimental autoimmune encephalitis—cytokine and hormonal correlates. Brain Behav. Immun. *33*, 164–172.

Anagnostaras, S.G., Gale, G.D., and Fanselow, M.S. (2001). Hippocampus and contextual fear conditioning: recent controversies and advances. Hippocampus *11*, 8–17.

Araque, A., Carmignoto, G., Haydon, P.G., Oliet, S.H., Robitaille, R., and Volterra, A. (2014). Gliotransmitters travel in time and space. Neuron *81*, 728–739.

Beattie, E.C., Stellwagen, D., Morishita, W., Bresnahan, J.C., Ha, B.K., Von Zastrow, M., Beattie, M.S., and Malenka, R.C. (2002). Control of synaptic strength by glial TNFalpha. Science *295*, 2282–2285.

Belarbi, K., Jopson, T., Tweedie, D., Arellano, C., Luo, W., Greig, N.H., and Rosi, S. (2012). TNF-α protein synthesis inhibitor restores neuronal function and reverses cognitive deficits induced by chronic neuroinflammation. J. Neuroinflammation *9*, 23.

Bezzi, P., Domercq, M., Brambilla, L., Galli, R., Schols, D., De Clercq, E., Vescovi, A., Bagetta, G., Kollias, G., Meldolesi, J., and Volterra, A. (2001). CXCR4-activated astrocyte glutamate release via TNFalpha: amplification by microglia triggers neurotoxicity. Nat. Neurosci. *4*, 702–710.

Centonze, D., Muzio, L., Rossi, S., Cavasinni, F., De Chiara, V., Bergami, A., Musella, A., D'Amelio, M., Cavallucci, V., Martorana, A., et al. (2009). Inflammation triggers synaptic alteration and degeneration in experimental autoimmune encephalomyelitis. J. Neurosci. *29*, 3442–3452.

Chapman, P.F., White, G.L., Jones, M.W., Cooper-Blacketer, D., Marshall, V.J., Irizarry, M., Younkin, L., Good, M.A., Bliss, T.V., Hyman, B.T., et al. (1999). Impaired synaptic plasticity and learning in aged amyloid precursor protein transgenic mice. Nat. Neurosci. *2*, 271–276.

Chiaravalloti, N.D., and DeLuca, J. (2008). Cognitive impairment in multiple sclerosis. Lancet Neurol. *7*, 1139–1151.

Clark, I.A., Alleva, L.M., and Vissel, B. (2010). The roles of TNF in brain dysfunction and disease. Pharmacol. Ther. *128*, 519–548.

Codarri, L., Gyülvészi, G., Tosevski, V., Hesske, L., Fontana, A., Magnenat, L., Suter, T., and Becher, B. (2011). RORγt drives production of the cytokine GM-CSF in helper T cells, which is essential for the effector phase of autoimmune neuroinflammation. Nat. Immunol. *12*, 560–567.

Cunningham, A.J., Murray, C.A., O'Neill, L.A., Lynch, M.A., and O'Connor, J.J. (1996). Interleukin-1 beta (IL-1 beta) and tumour necrosis factor (TNF) inhibit long-term potentiation in the rat dentate gyrus in vitro. Neurosci. Lett. *203*, 17–20.

Denny, C.A., Kheirbek, M.A., Alba, E.L., Tanaka, K.F., Brachman, R.A., Laughman, K.B., Tomm, N.K., Turi, G.F., Losonczy, A., and Hen, R. (2014). Hippocampal memory traces are differentially modulated by experience, time, and adult neurogenesis. Neuron *83*, 189–201.

Domercq, M., Brambilla, L., Pilati, E., Marchaland, J., Volterra, A., and Bezzi, P. (2006). P2Y1 receptor-evoked glutamate exocytosis from astrocytes: control by tumor necrosis factor-alpha and prostaglandins. J. Biol. Chem. *281*, 30684–30696.

Eugster, H.P., Frei, K., Bachmann, R., Bluethmann, H., Lassmann, H., and Fontana, A. (1999). Severity of symptoms and demyelination in MOG-induced EAE depends on TNFR1. Eur. J. Immunol. *29*, 626–632.

Gabbita, S.P., Srivastava, M.K., Eslami, P., Johnson, M.F., Kobritz, N.K., Tweedie, D., Greig, N.H., Zemlan, F.P., Sharma, S.P., and Harris-White, M.E. (2012). Early intervention with a small molecule inhibitor for tumor necrosis factor-α prevents cognitive deficits in a triple transgenic mouse model of Alzheimer's disease. J. Neuroinflammation *9*, 99.

Gold, S.M., Kern, K.C., O'Connor, M.F., Montag, M.J., Kim, A., Yoo, Y.S., Giesser, B.S., and Sicotte, N.L. (2010). Smaller cornu ammonis 2-3/dentate gyrus volumes and elevated cortisol in multiple sclerosis patients with depressive symptoms. Biol. Psychiatry *68*, 553–559.

Goussakov, I.V., Fink, K., Elger, C.E., and Beck, H. (2000). Metaplasticity of mossy fiber synaptic transmission involves altered release probability. J. Neurosci. *20*, 3434–3441.

Gregory, A.P., Dendrou, C.A., Attfield, K.E., Haghikia, A., Xifara, D.K., Butter, F., Poschmann, G., Kaur, G., Lambert, L., Leach, O.A., et al. (2012). TNF

Cell

receptor 1 genetic risk mirrors outcome of anti-TNF therapy in multiple sclerosis. Nature 488, 508–511.

Gu, Y., Arruda-Carvalho, M., Wang, J., Janoschka, S.R., Josselyn, S.A., Frankland, P.W., and Ge, S. (2012). Optical controlling reveals time-dependent roles for adult-born dentate granule cells. Nat. Neurosci. 15, 1700–1706.

Haji, N., Mandolesi, G., Gentile, A., Sacchetti, L., Fresegna, D., Rossi, S., Musella, A., Sepman, H., Motta, C., Studer, V., et al. (2012). TNF-alpha-mediated anxiety in a mouse model of multiple sclerosis. Exp. Neurol. 237, 296–303.

Halassa, M.M., Florian, C., Fellin, T., Munoz, J.R., Lee, S.Y., Abel, T., Haydon, P.G., and Frank, M.G. (2009). Astrocytic modulation of sleep homeostasis and cognitive consequences of sleep loss. Neuron 61, 213–219.

Han, J., Kesner, P., Metna-Laurent, M., Duan, T., Xu, L., Georges, F., Koehl, M., Abrous, D.N., Mendizabal-Zubiaga, J., Grandes, P., et al. (2012). Acute cannabinoids impair working memory through astroglial CB1 receptor modulation of hippocampal LTD. Cell 148, 1039–1050.

Han, X., Chen, M., Wang, F., Windrem, M., Wang, S., Shanz, S., Xu, Q., Oberheim, N.A., Bekar, L., Betstadt, S., et al. (2013). Forebrain engraftment by human glial progenitor cells enhances synaptic plasticity and learning in adult mice. Cell Stem Cell 12, 342–353.

He, P., Zhong, Z., Lindholm, K., Berning, L., Lee, W., Lemere, C., Staufenbiel, M., Li, R., and Shen, Y. (2007). Deletion of tumor necrosis factor death receptor inhibits amyloid beta generation and prevents learning and memory deficits in Alzheimer's mice. J. Cell Biol. 178, 829–841.

Hirrlinger, P.G., Scheller, A., Braun, C., Hirrlinger, J., and Kirchhoff, F. (2006). Temporal control of gene recombination in astrocytes by transgenic expression of the tamoxifen-inducible DNA recombinase variant CreERT2. Glia 54, 11–20.

Jourdain, P., Bergersen, L.H., Bhaukaurally, K., Bezzi, P., Santello, M., Domercq, M., Matute, C., Tonello, F., Gundersen, V., and Volterra, A. (2007). Glutamate exocytosis from astrocytes controls synaptic strength. Nat. Neurosci. 10, 331–339.

Kassiotis, G., and Kollias, G. (2001). Uncoupling the proinflammatory from the immunosuppressive properties of tumor necrosis factor (TNF) at the p55 TNF receptor level: implications for pathogenesis and therapy of autoimmune demyelination. J. Exp. Med. 193, 427–434.

Larsen, R.S., Corlew, R.J., Henson, M.A., Roberts, A.C., Mishina, M., Watanabe, M., Lipton, S.A., Nakanishi, N., Pérez-Otaño, I., Weinberg, R.J., and Philpot, B.D. (2011). NR3A-containing NMDARs promote neurotransmitter release and spike timing-dependent plasticity. Nat. Neurosci. 14, 338–344.

Lee, H.S., Ghetti, A., Pinto-Duarte, A., Wang, X., Dziewczapolski, G., Galimi, F., Huitron-Resendiz, S., Piña-Crespo, J.C., Roberts, A.J., Verma, I.M., et al. (2014). Astrocytes contribute to gamma oscillations and recognition memory. Proc. Natl. Acad. Sci. USA 111, E3343–E3352.

Liu, X., Ramirez, S., Pang, P.T., Puryear, C.B., Govindarajan, A., Deisseroth, K., and Tonegawa, S. (2012). Optogenetic stimulation of a hippocampal engram activates fear memory recall. Nature 484, 381–385.

McAlpine, F.E., and Tansey, M.G. (2008). Neuroinflammation and tumor necrosis factor signaling in the pathophysiology of Alzheimer's disease. J. Inflamm. Res. 1, 29–39.

Paoletti, P., Bellone, C., and Zhou, Q. (2013). NMDA receptor subunit diversity: impact on receptor properties, synaptic plasticity and disease. Nat. Rev. Neurosci. 14, 383–400.

Pascual, O., Casper, K.B., Kubera, C., Zhang, J., Revilla-Sanchez, R., Sul, J.Y., Takano, H., Moss, S.J., McCarthy, K., and Haydon, P.G. (2005). Astrocytic purinergic signaling coordinates synaptic networks. Science 310, 113–116.

Pribiag, H., and Stellwagen, D. (2013). TNF-α downregulates inhibitory neurotransmission through protein phosphatase 1-dependent trafficking of GABA(A) receptors. J. Neurosci. 33, 15879–15893.

Renno, T., Krakowski, M., Piccirillo, C., Lin, J.Y., and Owens, T. (1995). TNF-alpha expression by resident microglia and infiltrating leukocytes in the central nervous system of mice with experimental allergic encephalomyelitis. Regulation by Th1 cytokines. J. Immunol. 154, 944–953.

Rothe, J., Lesslauer, W., Lötscher, H., Lang, Y., Koebel, P., Köntgen, F., Althage, A., Zinkernagel, R., Steinmetz, M., and Bluethmann, H. (1993). Mice lacking the tumour necrosis factor receptor 1 are resistant to TNF-mediated toxicity but highly susceptible to infection by Listeria monocytogenes. Nature 364, 798–802.

Santello, M., and Volterra, A. (2012). TNFα in synaptic function: switching gears. Trends Neurosci. 35, 638–647.

Santello, M., Bezzi, P., and Volterra, A. (2011). TNFα controls glutamatergic gliotransmission in the hippocampal dentate gyrus. Neuron 69, 988–1001.

Srinivas, S., Watanabe, T., Lin, C.S., William, C.M., Tanabe, Y., Jessell, T.M., and Costantini, F. (2001). Cre reporter strains produced by targeted insertion of EYFP and ECFP into the ROSA26 locus. BMC Dev. Biol. 1, 4.

Stellwagen, D., Beattie, E.C., Seo, J.Y., and Malenka, R.C. (2005). Differential regulation of AMPA receptor and GABA receptor trafficking by tumor necrosis factor-alpha. J. Neurosci. 25, 3219–3228.

Suzuki, A., Stern, S.A., Bozdagi, O., Huntley, G.W., Walker, R.H., Magistretti, P.J., and Alberini, C.M. (2011). Astrocyte-neuron lactate transport is required for long-term memory formation. Cell 144, 810–823.

Swardfager, W., and Black, S.E. (2013). Dementia: A link between microbial infection and cognition? Nat. Rev. Neurol. 9, 301–302.

Terrando, N., Monaco, C., Ma, D., Foxwell, B.M., Feldmann, M., and Maze, M. (2010). Tumor necrosis factor-alpha triggers a cytokine cascade yielding postoperative cognitive decline. Proc. Natl. Acad. Sci. USA 107, 20518–20522.

Tombaugh, G.C., Rowe, W.B., Chow, A.R., Michael, T.H., and Rose, G.M. (2002). Theta-frequency synaptic potentiation in CA1 in vitro distinguishes cognitively impaired from unimpaired aged Fischer 344 rats. J. Neurosci. 22, 9932–9940.

Toni, N., Teng, E.M., Bushong, E.A., Aimone, J.B., Zhao, C., Consiglio, A., van Praag, H., Martone, M.E., Ellisman, M.H., and Gage, F.H. (2007). Synapse formation on neurons born in the adult hippocampus. Nat. Neurosci. 10, 727–734.

Van Hauwermeiren, F., Vandenbroucke, R.E., and Libert, C. (2011). Treatment of TNF mediated diseases by selective inhibition of soluble TNF or TNFR1. Cytokine Growth Factor Rev. 22, 311–319.

Victoratos, P., Lagnel, J., Tzima, S., Alimzhanov, M.B., Rajewsky, K., Pasparakis, M., and Kollias, G. (2006). FDC-specific functions of p55TNFR and IKK2 in the development of FDC networks and of antibody responses. Immunity 24, 65–77.

Wang, S., Ota, S., Guo, B., Ryu, J., Rhodes, C., Xiong, Y., Kalim, S., Zeng, L., Chen, Y., Teitell, M.A., and Zhang, X. (2011). Subcellular resolution mapping of endogenous cytokine secretion by nano-plasmonic-resonator sensor array. Nano Lett. 11, 3431–3434.

Xu, Z.Z., Zhang, L., Liu, T., Park, J.Y., Berta, T., Yang, R., Serhan, C.N., and Ji, R.R. (2010). Resolvins RvE1 and RvD1 attenuate inflammatory pain via central and peripheral actions. Nat. Med. 16, 592–597.

Yang, G., Parkhurst, C.N., Hayes, S., and Gan, W.B. (2013). Peripheral elevation of TNF-α leads to early synaptic abnormalities in the mouse somatosensory cortex in experimental autoimmune encephalomyelitis. Proc. Natl. Acad. Sci. USA 110, 10306–10311.

Yirmiya, R., and Goshen, I. (2011). Immune modulation of learning, memory, neural plasticity and neurogenesis. Brain Behav. Immun. 25, 181–213.